Journal of
Mechanics of
Materials and Structures

# GENERALIZED PLANE STRAIN FINITE-ELEMENT FORMULATION FOR THERMAL AND ELECTRICAL BUCKLING ANALYSIS OF PIEZO COMPOSITE BEAM

R. Jerome and N. Ganesan

Volume 3, Nº 9 November 2008

mathematical sciences publishers

JOURNAL OF MECHANICS OF MATERIALS AND STRUCTURES
Vol. 3, No. 9, 2008

# GENERALIZED PLANE STRAIN FINITE-ELEMENT FORMULATION FOR THERMAL AND ELECTRICAL BUCKLING ANALYSIS OF PIEZO COMPOSITE BEAM

R. JEROME AND N. GANESAN

We develop a generalized plane strain (GPS) finite element formulation to predict the critical buckling voltage and temperature of a piezo composite beam in more generality than the cases characterized by plane strain and plane stress assumptions.

This generalized plane strain formulation represents the two-dimensional finite element model as closely as possible to the three-dimensional finite element model. It is similar to the plane strain formulation that reduces a three-dimensional stress-strain relation to a two-dimensional one, but in contrast with most GPS formulations in the literature, it does not include out of plane degrees of freedom. In our formulation the reduced two-dimensional stress-strain relation incorporates the effect of allowed/applied strain $\varepsilon_0$ in the dimension not included in the two-dimensional model. Further, since the goal is to deal with thermal and electrical buckling analysis, an initial strain vector is incorporated in the formulation.

A finite element solver based on an eight-node quadrilateral element was developed under the new formulation, and its results show good agreement with those reported by Varelis and Saravanos (2004) and those obtained with ANSYS. The critical electrical and thermal buckling loads for examples other than those characterized by plane stress and plane strain were analyzed, and it was found that they are significantly influenced by $\alpha$, the parameter controlling the out-of-plane strains.

## 1. Introduction

Finite element analysis of smart structures has attracted much attention in recent years due to its wide range of applications. A significant amount of research has gone into the analysis of piezo composite structures. A number of finite element (FE) models have been proposed for the analysis of smart structures; and a detailed survey is given in [Benjeddou 2000]. One of the main problems addressed is the buckling analysis of smart structures.

Three-dimensional beam models can be simulated using two-dimensional in-plane elements by considering only the longitudinal cross-section of the three-dimensional beam model. The boundary conditions and the loading conditions can be simulated more accurately in this two-dimensional model than in the one-dimensional beam element model. Still, the two-dimensional analysis of the beam is based on either the plane stress or plane strain assumption, and cases outside these assumptions cannot be handled by two-dimensional in-plane elements. The generalized plane strain formulation can be used to model cases other than plane stress and plane strain at the cost of additional degrees of freedom.

The generalized plane strain formulation has been discussed extensively in the literature and has been used for several applications. Most composite problems are generalized plane strain in nature, and they

*Keywords:* generalized plane strain, finite element, piezo composite, beam, electrical buckling, thermal buckling.

are often solved using three-dimensional finite element analysis. Lin and Yi [1991] used the generalized plane strain formulation for the analysis of interlaminar stresses in viscoelastic composites. Krueger et al. [2002] have critically compared the two-dimensional finite element modeling assumptions with results from three-dimensional finite element analysis for composite skin-stiffener debonding. They have proposed a method for analyzing the composite using one layer of brick elements instead of using plane elements. Hu and Pagano [1997] presented a new method of solving generalized plane strain problems by introducing out-of-plane thermal strains in a two-dimensional finite element analysis with the plane strain model. They have done their proposed two-dimensional FE analysis using ANSYS and compared the results and computation time with those of the three-dimensional FE models.

In most of the literature, a plate element has been used to model the piezo composite plate as well as piezo composite beams for buckling analysis. Varelis and Saravanos [2002] developed a nonlinear mechanics to describe piezoelectric laminated plates, including nonlinear effects due to large displacements and rotations, and carried out a linear buckling analysis of plates by neglecting the nonlinear stiffness matrix. Varelis and Saravanos [2004] carried out pre- and post-buckling analysis of plates. Giannopoulos et al. [2007] presented a coupled formulation between thermal, electrical, and mechanical fields incorporating nonlinearity due to large displacements, and solved for linear buckling by neglecting the nonlinear stiffness matrix.

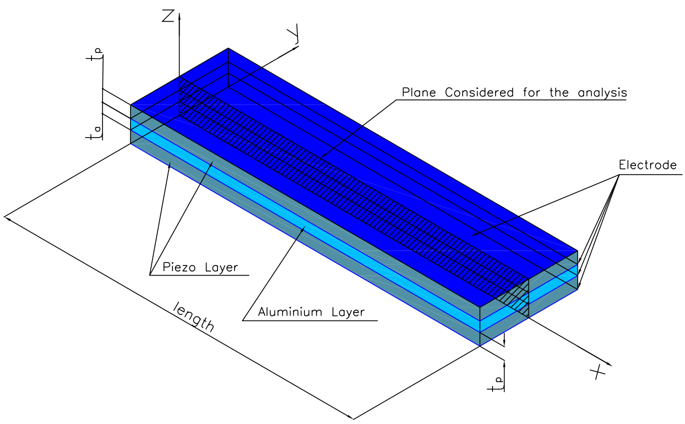


**Figure 1.** The three-dimensional piezo composite beam.

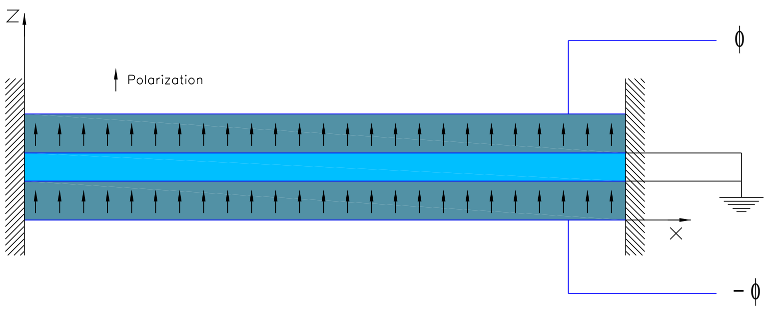


**Figure 2.** The plane of the finite element model used for thermal and electrical buckling analysis, with electrical boundary conditions and kinematic constraints. For thermal buckling analysis, the applied voltage is zero.

This paper presents a generalized plane strain FE formulation for thermal and electrical buckling of a piezo composite beam (Figure 1). The two-dimensional model is a cross-sectional one, as shown in Figure 2. This contrasts with the plate finite elements generally used to model a piezo composite beam [Varelis and Saravanos 2002; 2004; Giannopoulos et al. 2007]. Our generalized plane strain formulation is similar to the standard plane strain formulation (which reduces a three-dimensional stress-strain relation to a two-dimensional stress-strain relation), in that it does not include out-of-plane degrees of freedom. Therefore, it has fewer degrees of freedom than the conventional generalized plane strain formulation. As we shall see, however, this does not compromise its performance.

Our formulation includes the effect of out-of-plane strain (that is, in the direction not included in the two-dimensional FE model) via a parameter $\alpha$, which intervenes in the stress-strain relationship of the beam. The effect of the out-of-plane strain is included in the formulation through the constitutive relations.

We compare the performance of the plane strain model, the plane stress model and the newly developed generalized plane strain model in calculating the critical buckling voltage and critical buckling temperature of a piezo composite beam. It turns out that the present model simulates the three-dimensional FE model more closely than the conventional plane stress or plane strain two-dimensional FE model for the same number of degrees of freedom.

The present formulation can be used to analyze beams inside a gap or a slot which constrains expansion of the beam in the direction not included in the two-dimensional FE model.

***List of symbols***

| | |
|---|---|
| $\varepsilon_{xx}, \varepsilon_{yy}, \varepsilon_{zz}$ | Strains in the $x$, $y$ and $z$ directions |
| $\sigma_{xx}, \sigma_{yy}, \sigma_{zz}$ | Stresses in the $x$, $y$ and $z$ directions |
| $\varepsilon_{x0}, \varepsilon_{y0}, \varepsilon_{z0}$ | Initial strains in the $x$, $y$ and $z$ directions |
| $\varepsilon_{yy}^{0}$ | Free expansion strain in $y$ direction |
| $\sigma_{yy}^{\mathrm{PS}}$ | Stress in the $y$ direction for plane strain case |
| $\sigma_{yy}^{G}$ | Stress in the $y$ direction for generalized plane strain |
| $\varepsilon^{0}$ | allowed/applied strain in the $z$ direction |
| $\alpha = \varepsilon^{0}/\varepsilon_{yy}^{0}$ | Ratio between allowed/applied strain to the free expansion strain in the $z$ direction |
| $\{T\}$ | Stress vector |
| $\{S\}$ | Stain vector |
| $\{S_0\}$ | Initial strain vector |
| $\{E\}$ | Electric field vector |
| $\{D\}$ | Electric displacement vector |
| $[c]$, $[s]$ | Elastic constants matrices |
| $[\varepsilon]$ | Dielectric constants matrix |
| $[d]$, $[e]$ | Piezoelectric constants matrix |
| $[\bar{c}]$, $[\bar{s}]$ | two-dimensional reduced elastic constants matrices |
| $[\bar{\varepsilon}]$ | two-dimensional reduced dielectric constants matrix |
| $[\bar{d}]$, $[\bar{e}]$ | two-dimensional reduced piezoelectric constants matrix |
| $\{u_e\}$ | Elemental structural displacement degrees of freedom |
| $\{\varphi_e\}$ | Elemental electric potential degrees of freedom |

| | |
|---|---|
| $[N_u]$ | Shape function matrix for structural displacement |
| $[N_\varphi]$ | Shape function matrix for electric potential |
| $[B_u]$ | Shape function derivative matrix for structural strain |
| $[B_\phi]$ | Shape function derivative matrix for electric field |
| $[M]$ | Elemental mass matrix |
| $[K_{uu}]$ | Elemental structural stiffness matrix |
| $[K_{u\varphi}]$ | Elemental piezostructure coupling matrix |
| $[K_{\varphi\varphi}]$ | Elemental capacitance matrix |
| $\{f_e\}$ | Elemental external mechanical force |
| $\{g_e\}$ | Elemental electrical charge |
| $[K_\sigma]$ | Elemental geometric nonlinear matrix |
| $s$ | Elemental stress matrix |
| $[M]$ | Assembled mass matrix |
| $[\boldsymbol{K}_{uu}]$ | Assembled structural stiffness matrix |
| $[\boldsymbol{K}_{u\varphi}]$ | Assembled piezostructure coupling matrix |
| $[\boldsymbol{K}_{\varphi\varphi}]$ | Assembled capacitance matrix |
| $[\boldsymbol{K}_\sigma]$ | Assembled geometric nonlinear matrix |
| $\{\boldsymbol{f}\}$ | Assembled external mechanical force |
| $[\boldsymbol{K}_{\mathrm{eq}}]$ | Assembled equivalent capacitance matrix |

## 2. Formulation

***Generalized plane strain FE formulation.*** The three-dimensional stress-strain relation is given by

$$\varepsilon_{xx} = s_{11}\sigma_{xx} + s_{12}\sigma_{yy} + s_{13}\sigma_{zz} + \varepsilon_{x0}, \tag{1}$$

$$\varepsilon_{yy} = s_{21}\sigma_{xx} + s_{22}\sigma_{yy} + s_{23}\sigma_{zz} + \varepsilon_{y0}, \tag{2}$$

$$\varepsilon_{zz} = s_{31}\sigma_{xx} + s_{32}\sigma_{yy} + s_{33}\sigma_{zz} + \varepsilon_{z0}, \tag{3}$$

where $\varepsilon_{xx}$, $\varepsilon_{yy}$ and $\varepsilon_{zz}$ are the strains in the $x$, $y$ and $z$ directions and $\sigma_{xx}$, $\sigma_{yy}$ and $\sigma_{zz}$ are the stresses in the $x$, $y$ and $z$ directions. The strains $\varepsilon_{x0}$, $\varepsilon_{y0}$ and $\varepsilon_{z0}$ are the initial strains. Consider a plane strain case where $\varepsilon_{yy} = \gamma_{xy} = \gamma_{yz} = 0$. Because of the assumption $\varepsilon_{yy} = 0$, Equation (3) becomes $\varepsilon_{yy} = s_{21}\sigma_{xx} + s_{22}\sigma_{yy} + s_{23}\sigma_{zz} + \varepsilon_{y0} = 0$, which gives

$$\sigma_{yy} = -\frac{s_{21}}{s_{22}}\sigma_{xx} - \frac{s_{23}}{s_{22}}\sigma_{zz} - \frac{\varepsilon_{y0}}{s_{22}}. \tag{4}$$

This $\sigma_{yy}$ is required to resist the $y$ direction strain $\varepsilon^0_{yy}$ caused by the stresses $\sigma_{xx}$ and $\sigma_{zz}$. Therefore, $\sigma_{yy}$ produces a strain equal to $\varepsilon^0_{yy}$ but in the opposite direction, so the net strain in the $y$ direction is maintained at zero.

Based on this argument, Equation (4) can be recast as

$$s_{22}\sigma_{yy} = -\varepsilon^0_{yy} = -s_{21}\sigma_{xx} - s_{23}\sigma_{zz} - \varepsilon_{y0}. \tag{5}$$

Substituting $\sigma_{yy}$ from (4) into (1) and (2) for the plane strain case implies, from (5), that we are incorporating the effect of $-\varepsilon^0_{yy}$ in the two-dimensional stress-strain relation. The stress-strain relationship then becomes

$$\begin{Bmatrix} \varepsilon_{xx} \\ \varepsilon_{zz} \\ \gamma_{xz} \end{Bmatrix} = \begin{bmatrix} s_{11} - s_{12}^2/s_{22} & s_{13} - s_{12}s_{23}/s_{22} & 0 \\ s_{13} - s_{12}s_{23}/s_{22} & s_{33} - s_{23}^2/s_{22} & 0 \\ 0 & 0 & s_{55} \end{bmatrix} \begin{Bmatrix} \sigma_{xx} \\ \sigma_{zz} \\ \tau_{xz} \end{Bmatrix} + \begin{Bmatrix} \varepsilon_{x0} - (s_{12}/s_{22})\varepsilon_{y0} \\ \varepsilon_{z0} - (s_{23}/s_{22})\varepsilon_{y0} \\ \gamma_{xz0} \end{Bmatrix}, \tag{6}$$

which enforces the condition $\varepsilon_{yy} = 0$.

Now consider the case where $\varepsilon_{yy} = \varepsilon_{yy}^0$ but $\gamma_{xy} = \gamma_{yz} = 0$, that is, the $y$ direction is allowed to expand freely, as shown in Figure 3. In this case the effect of $\varepsilon_{yy}^0$ caused by the stresses $\sigma_{xx}$ and $\sigma_{zz}$ has to be incorporated into the two-dimensional stress-strain relation. From (5), it is clear that to produce positive strain $\varepsilon_{yy}^0$, the stress $\sigma_{yy}$ should be in the opposite direction of the plane strain case. From (5) we get

$$s_{22}\sigma_{yy}^G = s_{22}\left(-\sigma_{yy}^{\mathrm{PS}}\right) = \varepsilon_{yy}^0 = s_{21}\sigma_{xx} + s_{23}\sigma_{zz} + \varepsilon_{y0}, \tag{7}$$

$$\sigma_{yy}^G = \left(-\sigma_{yy}^{\mathrm{PS}}\right) = \frac{s_{21}}{s_{22}}\sigma_{xx} + \frac{s_{23}}{s_{22}}\sigma_{zz} + \frac{\varepsilon_{y0}}{s_{22}}, \tag{8}$$

where $\sigma_{yy}^G$ and $\sigma_{yy}^{\mathrm{PS}}$ are the stresses in the $y$ direction for the case $\varepsilon_{yy} = \varepsilon_{yy}^0$ and for the plane strain case, respectively.

By substituting $\sigma_{yy}^G$ from (8) into (1) and (2), we obtain for the stress-strain relationship the equation

$$\begin{Bmatrix} \varepsilon_{xx} \\ \varepsilon_{zz} \\ \gamma_{xz} \end{Bmatrix} = \begin{bmatrix} s_{11} + s_{12}^2/s_{22} & s_{13} + s_{12}s_{23}/s_{22} & 0 \\ s_{13} + s_{12}s_{23}/s_{22} & s_{33} + s_{23}^2/s_{22} & 0 \\ 0 & 0 & s_{55} \end{bmatrix} \begin{Bmatrix} \sigma_{xx} \\ \sigma_{zz} \\ \tau_{xz} \end{Bmatrix} + \begin{Bmatrix} \varepsilon_{x0} + (s_{12}/s_{22})\varepsilon_{y0} \\ \varepsilon_{z0} + (s_{23}/s_{22})\varepsilon_{y0} \\ \gamma_{xz0} \end{Bmatrix}, \tag{9}$$

which enforces the condition $\varepsilon_{yy} = \varepsilon_{yy}^0$.

Before enforcing this condition, however, the condition $\varepsilon_{yy} = 0$ has to be enforced, which means that before applying the strain $\varepsilon_{yy}^0$, there should not be any strain in the $y$ direction. By enforcing the

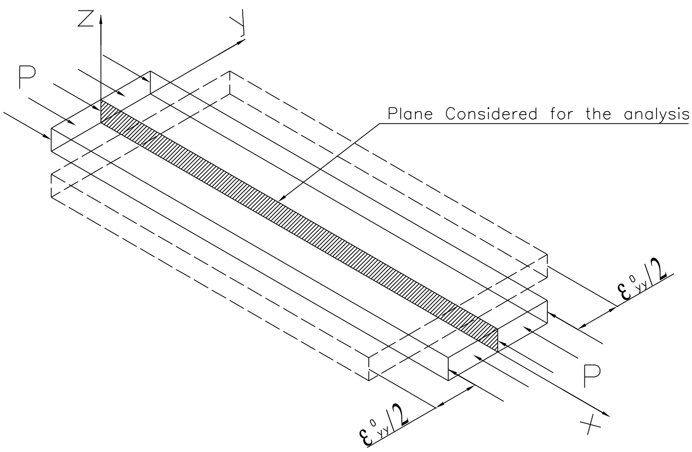


**Figure 3.** The beam is allowed to expand freely in $y$ direction.

condition $\varepsilon_{yy}=0$, the stress-strain relation becomes (6). Introducing the quantities

$$s'_{11}=s_{11}-\frac{s_{12}^2}{s_{22}},\quad s'_{13}=s_{13}-\frac{s_{12}s_{23}}{s_{22}},\quad s'_{33}=s_{33}-\frac{s_{23}^2}{s_{22}},\quad \varepsilon'_{x0}=\varepsilon_{x0}-\frac{s_{12}}{s_{22}}\varepsilon_{y0},\quad \varepsilon'_{z0}=\varepsilon_{z0}-\frac{s_{23}}{s_{22}}\varepsilon_{y0},\tag{10}$$

we can recast (6) as

$$\begin{Bmatrix}\varepsilon_{xx}\\ \varepsilon_{zz}\\ \gamma_{xz}\end{Bmatrix}=\begin{bmatrix}s'_{11} & s'_{13} & 0\\ s'_{13} & s'_{33} & 0\\ 0 & 0 & s_{55}\end{bmatrix}\begin{Bmatrix}\sigma_{xx}\\ \sigma_{zz}\\ \tau_{xz}\end{Bmatrix}+\begin{Bmatrix}\varepsilon'_{x0}\\ \varepsilon'_{z0}\\ \gamma_{xz0}\end{Bmatrix}.\tag{11}$$

Next, the condition $\varepsilon_{yy}=\varepsilon_{yy}^0$ has to be enforced on the $y$ direction for the strain-free ($\varepsilon_{yy}=0$) stress-strain relation. By enforcing the condition $\varepsilon_{yy}=\varepsilon_{yy}^0$, the stress-strain relation becomes (9) . Now the stress-strain relation becomes

$$\begin{Bmatrix}\varepsilon_{xx}\\ \varepsilon_{zz}\\ \gamma_{xz}\end{Bmatrix}=\begin{bmatrix}s'_{11}+s_{12}^2/s_{22} & s'_{13}+s_{12}s_{23}/s_{22} & 0\\ s'_{13}+s_{12}s_{23}/s_{22} & s'_{33}+s_{23}^2/s_{22} & 0\\ 0 & 0 & s_{55}\end{bmatrix}\begin{Bmatrix}\sigma_{xx}\\ \sigma_{zz}\\ \tau_{xz}\end{Bmatrix}+\begin{Bmatrix}\varepsilon'_{x0}+(s_{12}/s_{22})\varepsilon_{y0}\\ \varepsilon'_{z0}+(s_{23}/s_{22})\varepsilon_{y0}\\ \gamma_{xz0}\end{Bmatrix}\tag{12}$$

The two conditions $\varepsilon_{yy}=0$ and $\varepsilon_{yy}=\varepsilon_{yy}^0$ can be enforced in any order; this is just a superposition of one condition over the other. The condition $\varepsilon_{yy}=0$ enforces zero strain in the $y$ direction, and $\varepsilon_{yy}=\varepsilon_{yy}^0$ says the beam can expand freely in the $y$ direction. By superimposing these two conditions, the beam is forced to expand exactly the same amount as that of free expansion in the $y$ direction. The derivation for generalized plane strain is carried out based on this analogy.

For the generalized plane strain case we have $\varepsilon_{yy}=\varepsilon^0$ but $\gamma_{xy}=\gamma_{yz}=0$. In this case, $\varepsilon^0$ is the allowed/applied strain in the $y$ direction. If $\varepsilon^0$ is specified as a multiple of $\varepsilon_{yy}^0$, its effect can be taken into account in the two-dimensional stress-strain relation.

Let the allowed/applied strain be $\varepsilon^0=\alpha\varepsilon_{yy}^0$, as shown in Figures 4 and 5. The reduced two-dimensional stress-strain relation, incorporating the effect of $\varepsilon^0$, becomes

$$\begin{Bmatrix}\varepsilon_{xx}\\ \varepsilon_{zz}\\ \gamma_{xz}\end{Bmatrix}=\begin{bmatrix}s'_{11}+\alpha s_{12}^2/s_{22} & s'_{13}+\alpha s_{12}s_{23}/s_{22} & 0\\ s'_{13}+\alpha s_{12}s_{23}/s_{22} & s'_{33}+\alpha s_{23}^2/s_{22} & 0\\ 0 & 0 & s_{55}\end{bmatrix}\begin{Bmatrix}\sigma_{xx}\\ \sigma_{zz}\\ \tau_{xz}\end{Bmatrix}+\begin{Bmatrix}\varepsilon'_{x0}+\alpha(s_{12}/s_{22})\varepsilon_{y0}\\ \varepsilon'_{z0}+\alpha(s_{23}/s_{22})\varepsilon_{y0}\\ \gamma_{xz0}\end{Bmatrix},\tag{13}$$

where $s'_{11}$, $s'_{12}$, and $s'_{22}$ are given by (10) .

If $\alpha$ in (13) is 0, then (13) reduces to (6), which is a stress-strain relation for the plane strain case. If the $\alpha$ in (13) is 1, then (13) reduces to (12), which is a stress-strain relation for the condition $\varepsilon_{yy}=\varepsilon_{yy}^0$. By substituting (10) into (12) , the stress-strain relation for the condition $\varepsilon_{yy}=\varepsilon_{yy}^0$ becomes

$$\begin{Bmatrix}\varepsilon_{xx}\\ \varepsilon_{zz}\\ \gamma_{xz}\end{Bmatrix}=\begin{bmatrix}s_{11} & s_{13} & 0\\ s_{13} & s_{33} & 0\\ 0 & 0 & s_{55}\end{bmatrix}\begin{Bmatrix}\sigma_{xx}\\ \sigma_{zz}\\ \tau_{xz}\end{Bmatrix}+\begin{Bmatrix}\varepsilon_{x0}\\ \varepsilon_{z0}\\ \gamma_{xz0}\end{Bmatrix}.\tag{14}$$

This is a simple two-dimensional stress-strain relation which completely does not constrain the strain $\varepsilon_{yy}^0$, caused by the stresses $\sigma_{xx}$ and $\sigma_{zz}$.

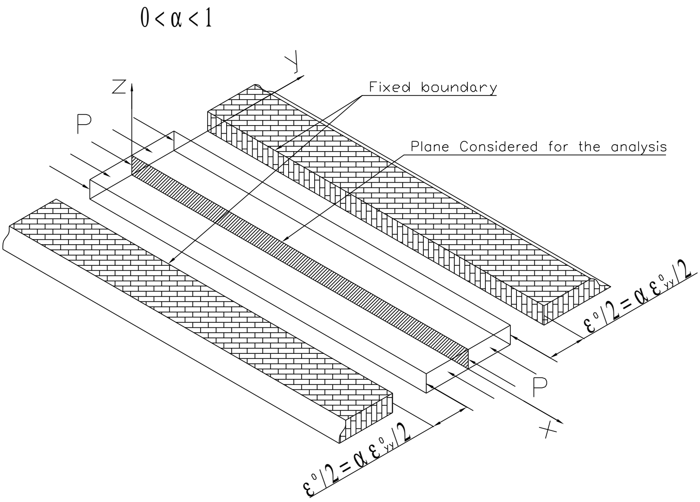


**Figure 4.** Beam is not allowed to undergo full free expansion in the $y$ direction.

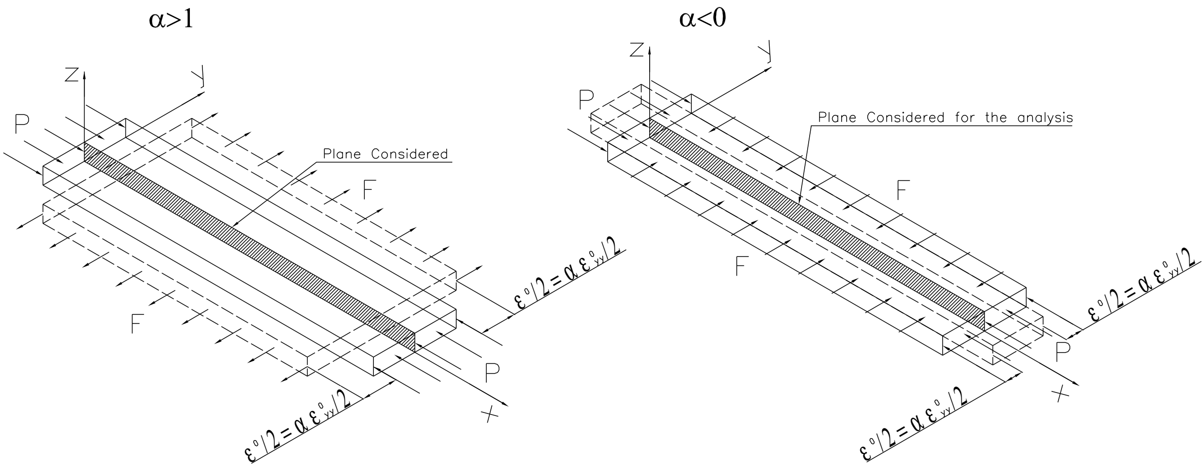


**Figure 5.** Left: Beam expands more than the free expansion in the $y$ direction by the external load. Right: Beam gets compressed in the $y$ direction by the external load.

The generalized plane strain stress-strain relations of (13) can be extended to generalized plane strain two-dimensional piezostructure coupled stress-strain relations. The constitutive equations for a piezoelectric material are

$$\{T\} = [c^E]\big(\{S\} - \{S_0\}\big) - [e]^T\{E\}, \quad \{D\} = [e]\{S\} + [\varepsilon^S]\{E\}, \tag{15}$$

where $\{T\}$ is the stress vector, $\{S\}$ the stain vector, $\{S_0\}$ the initial strain vector, $\{E\}$ the electric field vector, $\{D\}$ the electric displacement vector, $[c]$ and $[s]$ the elastic constants matrices, $[\varepsilon]$ the dielectric constants matrix, and $[d]$ and $[e]$ the piezoelectric constants matrix, and where superscript $E$ and $S$ indicate that the specified values are evaluated at constant $E$ and $S$.

Equation (15) can be written in strain form as

$$\{S\} = [s^E]\{T\} + [d]^T\{E\} + \{S_0\}, \quad \{D\} = [d]\{T\} + [\varepsilon^E]\{E\}, \tag{16}$$

where

$$[e] = [d][c^E], \quad [c^E] = [s^E]^{-1}. \tag{17}$$

Equation (16) can be recast as

$$\begin{Bmatrix} \{S\} \\ \{D\} \end{Bmatrix} = \begin{bmatrix} [s^E] & [d]^T \\ [d] & [\varepsilon^E] \end{bmatrix} \begin{Bmatrix} \{T\} \\ \{E\} \end{Bmatrix} + \begin{Bmatrix} \{S_0\} \\ \{0\} \end{Bmatrix}. \tag{18}$$

This in turn can be expanded for the case where the polarization direction is the positive $z$ axis as follows:

$$\begin{Bmatrix} S_1 \\ S_2 \\ S_3 \\ S_4 \\ S_5 \\ S_6 \\ D_1 \\ D_2 \\ D_3 \end{Bmatrix} = \begin{bmatrix} s_{11} & s_{12} & s_{13} & 0 & 0 & 0 & 0 & 0 & d_{31} \\ s_{12} & s_{22} & s_{23} & 0 & 0 & 0 & 0 & 0 & d_{32} \\ s_{13} & s_{23} & s_{33} & 0 & 0 & 0 & 0 & 0 & d_{33} \\ 0 & 0 & 0 & s_{44} & 0 & 0 & 0 & d_{24} & 0 \\ 0 & 0 & 0 & 0 & s_{55} & 0 & d_{15} & 0 & 0 \\ 0 & 0 & 0 & 0 & 0 & s_{66} & 0 & 0 & 0 \\ 0 & 0 & 0 & 0 & d_{15} & 0 & \varepsilon_{11} & 0 & 0 \\ 0 & 0 & 0 & d_{24} & 0 & 0 & 0 & \varepsilon_{22} & 0 \\ d_{31} & d_{32} & d_{33} & 0 & 0 & 0 & 0 & 0 & \varepsilon_{33} \end{bmatrix} \begin{Bmatrix} T_1 \\ T_2 \\ T_3 \\ T_4 \\ T_5 \\ T_6 \\ E_1 \\ E_2 \\ E_3 \end{Bmatrix} + \begin{Bmatrix} S_{10} \\ S_{20} \\ S_{30} \\ S_{40} \\ S_{50} \\ S_{60} \\ 0 \\ 0 \\ 0 \end{Bmatrix}. \tag{19}$$

In the piezostructure coupled two-dimensional case, the $xz$ plane is considered for analysis as shown in Figure 2, and the $y$ direction is the be the out-of-plane direction. Now consider the plane strain case, where

$$S_2 = S_4 = S_6 = 0, \tag{20}$$

$$D_2 = E_2 = 0. \tag{21}$$

By substituting (20) into (19) , the second row of (19) becomes $S_2 = s_{12}T_1 + s_{22}T_2 + s_{23}T_3 + d_{32}E_3 + S_{20} = 0$, which gives

$$T_2 = -\frac{s_{12}}{s_{22}}T_1 - \frac{s_{23}}{s_{22}}T_3 - \frac{d_{32}}{s_{22}}E_3 - \frac{S_{20}}{s_{22}}. \tag{22}$$

Substituting (22) into (19) and using (20) and (21), we obtain the reduced stress-strain relationship in the plane strain case in the form

$$\begin{Bmatrix} S_1 \\ S_3 \\ S_5 \\ D_1 \\ D_3 \end{Bmatrix} = \begin{bmatrix} s'_{11} & s'_{13} & 0 & 0 & d'_{31} \\ s'_{13} & s'_{33} & 0 & 0 & d'_{33} \\ 0 & 0 & s_{55} & d_{15} & 0 \\ 0 & 0 & d_{15} & \varepsilon_{11} & 0 \\ d'_{31} & d'_{33} & 0 & 0 & \varepsilon'_{33} \end{bmatrix} \begin{Bmatrix} T_1 \\ T_3 \\ T_5 \\ E_1 \\ E_3 \end{Bmatrix} + \begin{Bmatrix} S'_{10} \\ S'_{30} \\ S_{50} \\ 0 \\ 0 \end{Bmatrix}, \tag{23}$$

where

$$s'_{11}=s_{11}-\frac{s_{12}^2}{s_{22}},\qquad s'_{13}=s_{13}-\frac{s_{12}s_{23}}{s_{22}},\qquad s'_{33}=s_{33}-\frac{s_{23}^2}{s_{22}},\tag{24}$$

$$d'_{31}=d_{31}-\frac{s_{12}d_{32}}{s_{22}},\qquad d'_{33}=d_{33}-\frac{s_{23}d_{32}}{s_{22}},\qquad \varepsilon'_{33}=\varepsilon_{33}-\frac{d_{32}^2}{s_{22}},\tag{25}$$

$$S'_{10}=S_{10}-\frac{s_{12}}{s_{22}}S_{20},\qquad S'_{30}=S_{30}-\frac{s_{23}}{s_{22}}S_{20}.\tag{26}$$

The arguments given for the pure elastic generalized plane strain case can be extended for the piezo-structure coupled generalized plane strain case. The reduced two-dimensional piezostructure coupled stress-strain relationship for the generalized plane strain case is given by

$$\begin{Bmatrix}S_1\\S_3\\S_5\\D_1\\D_3\end{Bmatrix}=\begin{bmatrix}s'_{11}+\alpha s_{12}^2/s_{22} & s'_{13}+\alpha s_{12}s_{23}/s_{22} & 0 & 0 & d'_{31}+\alpha s_{12}d_{32}/s_{22}\\ s'_{13}+\alpha s_{12}s_{23}/s_{22} & s'_{33}+\alpha s_{23}^2/s_{22} & 0 & 0 & d'_{33}+\alpha s_{23}d_{32}/s_{22}\\ 0 & 0 & s_{55} & d_{15} & 0\\ 0 & 0 & d_{15} & \varepsilon_{11} & 0\\ d'_{31}+\alpha s_{12}d_{32}/s_{22} & d'_{33}+\alpha s_{23}d_{32}/s_{22} & 0 & 0 & \varepsilon'_{33}+\alpha d_{32}^2/s_{22}\end{bmatrix}\begin{Bmatrix}T_1\\T_3\\T_5\\E_1\\E_3\end{Bmatrix}+\begin{Bmatrix}S'_{10}-\alpha s_{12}S_{20}/s_{22}\\S'_{30}-\alpha s_{23}S_{20}/s_{22}\\S_{50}\\0\\0\end{Bmatrix},$$

which can be recast as

$$\begin{Bmatrix}\{S\}\\\{D\}\end{Bmatrix}=\begin{bmatrix}[\bar{s}] & [\bar{d}]^T\\ [\bar{d}] & [\bar{\varepsilon}\ ]\end{bmatrix}\begin{Bmatrix}\{T\}\\\{E\}\end{Bmatrix}+\begin{Bmatrix}\{\overline{S}_0\}\\\{0\}\end{Bmatrix},\qquad \{S\}=[\bar{s}]\{T\}+[\bar{d}]^T\{E\}+\{\overline{S}_0\},\qquad \{D\}=[\bar{d}]\{T\}+[\bar{\varepsilon}]\{E\}.$$

Using (17) , this can further be rewritten in stress form as

$$\{T\}=[\bar{c}]\left(\{S\}-\left\{\overline{S_0}\right\}\right)-[\bar{e}]^T\{E\},\qquad \{D\}=[\bar{e}]\{S\}+[\bar{\varepsilon}]\{E\}.$$

***Finite element formulation.*** In order to model the piezo composite beam, an eight-node quadrilateral element was developed. The finite element model of the piezo composite beam is shown in Figure 6. Each node has three degrees of freedom: axial displacement ($u_1$), transverse displacement ($u_3$) and electric potential ($\phi$). The elemental degrees of freedom are

$$\{u_e\}=\left\{u_1^1,u_3^1,u_1^2,u_3^2,u_1^3,u_3^3,\ldots,u_1^8,u_3^8\right\}^T,\qquad \{\varphi_e\}=\{\varphi_1,\varphi_2,\varphi_3,\ldots,\varphi_8\}^T.\tag{27}$$

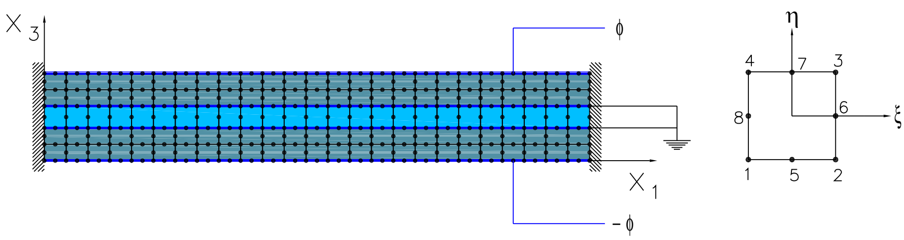


**Figure 6.** Finite element model of the piezo composite beam with kinematic constraints and electrical boundary conditions for electrical buckling analysis and (with zero applied voltage) for thermal buckling analysis.

The displacement $\{u\} = \{u_1, u_3\}^T$ and electric potential ($\phi$) within the element can be expressed in terms of element shape functions as

$$\{u\} = [N_u]\{u_e\}, \quad \{\varphi\} = [N_\varphi]\{\varphi_e\},$$

where

$$[N_u] = \begin{bmatrix} N_1 & 0 & N_2 & 0 & \dots & N_8 & 0 \\ 0 & N_1 & 0 & N_2 & \dots & 0 & N_8 \end{bmatrix}, \quad [N_\varphi] = [N_1 \;\; N_2 \;\; N_3 \;\; \dots \;\; N_8],$$

$N_1, N_2, \dots, N_8$ being the shape functions.

The strain displacement relation can be expressed as

$$\{S\} = \begin{Bmatrix} S_1 \\ S_3 \\ S_5 \end{Bmatrix} = \begin{Bmatrix} \partial u_1/\partial x_1 \\ \partial u_3/\partial x_3 \\ \partial u_1/\partial x_3 + \partial u_3/\partial x_1 \end{Bmatrix} = [B_u]\{u_e\},$$

where $[B_u]$ is the shape function derivative matrix:

$$[B_u] = \begin{bmatrix} \partial N_1/\partial x_1 & 0 & \partial N_2/\partial x_1 & 0 & \dots & \partial N_8/\partial x_1 & 0 \\ 0 & \partial N_1/\partial x_3 & 0 & \partial N_2/\partial x_3 & \dots & 0 & \partial N_8/\partial x_3 \\ \partial N_1/\partial x_3 & \partial N_1/\partial x_1 & \partial N_2/\partial x_3 & \partial N_2/\partial x_1 & \dots & \partial N_8/\partial x_3 & \partial N_8/\partial x_1 \end{bmatrix}$$

The electric field-potential relation can be expressed as

$$\{E\} = \begin{Bmatrix} E_1 \\ E_3 \end{Bmatrix} = \begin{Bmatrix} -\partial\varphi/\partial x_1 \\ -\partial\varphi/\partial x_3 \end{Bmatrix} = [B_\varphi]\{\varphi_e\},$$

where $[B_\phi]$ is the shape function derivative matrix:

$$[B_\varphi] = \begin{bmatrix} \partial N_1/\partial x_1 & \partial N_2/\partial x_1 & \partial N_3/\partial x_1 & \dots & \partial N_8/\partial x_1 \\ \partial N_1/\partial x_3 & \partial N_2/\partial x_3 & \partial N_3/\partial x_3 & \dots & \partial N_8/\partial x_3 \end{bmatrix}.$$

After application of the variational principle, the coupled finite element matrix equation becomes (see [Allik and Hughes 1970; Lerch 1990; Tzou and Tseng 1990])

$$[M]\{\ddot{u}_e\} + [K_{uu}]\{u_e\} + [K_{u\varphi}]\{\varphi_e\} = \{f_e\}, \quad [K_{\varphi u}]\{u_e\} + [K_{\varphi\varphi}]\{\varphi_e\} = \{g_e\}, \tag{28}$$

where $[M] = \int_V \rho [N]^T [N]\, dV$ is the element mass,

$$[K_{uu}] = \int_V [B_u]^T [\bar{c}^E][B_u]\, dV, \quad [K_{u\varphi}] = [K_{\varphi u}]^T = \int_V [B_u]^T [\bar{e}]^T [B_\varphi]\, dV, \quad [K_{\varphi\varphi}] = \int_V [B_\varphi]^T [\bar{\varepsilon}][B_\varphi]\, dV$$

are the stiffness, piezoelectric coupling and capacitance matrices, and

$$\{f_e\} = \int_V [B_u]^T [\bar{c}^E]\{S_0\}\, dV + \int_V [N]^T \{P_b\}\, dV + \int_{\Omega_1} [N]^T \{P_s\} d\Omega_1 + [N]^T \{P_c\}, \tag{29}$$

$$\{g_e\} = -\int_{\Omega_2} [N]^T P\, d\Omega_2 - [N]^T Q \tag{30}$$

are the external mechanical force and electrical charge. The first term in (29) is the element load vector due to initial strains, and the other terms are body, surface, and point forces, respectively [Cook et al. 2003].

In order to do the buckling analysis, the geometric nonlinear matrix can be computed as [Cook et al. 2003]

$$[K_\sigma] = \int_V [G]^T \begin{bmatrix} s & 0 \\ 0 & s \end{bmatrix} [G]\, dV,$$

where

$$s = \begin{bmatrix} \sigma_{x0} & \tau_{xz0} \\ \tau_{xz0} & \sigma_{z0} \end{bmatrix} \quad \text{and} \quad [G] = \begin{bmatrix} \partial N_1/\partial x_1 & 0 & \partial N_2/\partial x_1 & 0 & \dots & \partial N_8/\partial x_1 & 0 \\ \partial N_1/\partial x_3 & 0 & \partial N_2/\partial x_3 & 0 & \dots & \partial N_8/\partial x_3 & 0 \\ 0 & \partial N_1/\partial x_1 & 0 & \partial N_2/\partial x_1 & \dots & 0 & \partial N_8/\partial x_1 \\ 0 & \partial N_1/\partial x_3 & 0 & \partial N_2/\partial x_3 & \dots & 0 & \partial N_8/\partial x_3 \end{bmatrix}$$

are the stress and shape function derivative matrices.

For static analysis and for the case where only a mechanical load exists, Equation (28) becomes, after assembling the stiffness matrices,

$$[\boldsymbol{K}_{uu}]\{\boldsymbol{u}\} + [\boldsymbol{K}_{u\varphi}]\{\boldsymbol{\phi}\} = \{\boldsymbol{f}\}, \quad [\boldsymbol{K}_{\varphi u}]\{\boldsymbol{u}\} + [\boldsymbol{K}_{\varphi\varphi}]\{\boldsymbol{\phi}\} = 0; \tag{31}$$

the assembled geometric nonlinear matrix is $[\boldsymbol{K}_\sigma]$.

In the case of thermal buckling analysis, since only the thermal load exists, the right-hand side of $(31)_1$ is simply

$$\{\boldsymbol{f}\} = \sum \int_V [B_u]^T [\bar{c}^E]\{S_0\}\, dV,$$

and the assembled buckling eigenequation is

$$\big([\boldsymbol{K}_{uu}] + \lambda[\boldsymbol{K}_\sigma]\big)\{\delta\boldsymbol{u}\} = \{0\}. \tag{32}$$

In the case of electrical buckling analysis, the right-hand side of (31) is $\{\boldsymbol{f}\} = \{0\}$ and the known quantities are only the voltages on the electrodes. Therefore, for electrical buckling, (31) becomes

$$[\boldsymbol{K}_{uu}]\{\boldsymbol{u}\} + [\boldsymbol{K}_{u\varphi}]\{\boldsymbol{\phi}\} = \{0\}, \quad [\boldsymbol{K}_{\varphi u}]\{\boldsymbol{u}\} + [\boldsymbol{K}_{\varphi\varphi}]\{\boldsymbol{\phi}\} = \{0\}. \tag{33}$$

Since the FE model is a cross section model, as shown in Figure 6, the voltages are known only at the electrodes. There are other nodes in the piezo layer whose potentials have to be evaluated, and this in a coupled way. To evaluate the voltages applied in the piezolayer in a coupled way, Equation $(33)_1$ is solved for $\{\boldsymbol{u}\}$ and it is substituted into $(33)_2$ to get an equivalent stiffness matrix

$$[\boldsymbol{K}_{\text{eq}}] = [\boldsymbol{K}_{\varphi\varphi}] + [\boldsymbol{K}_{\varphi u}][\boldsymbol{K}_{uu}]^{-1}(-[\boldsymbol{K}_{u\varphi}].)$$

Now $[\boldsymbol{K}_{\text{eq}}]$ is a coupled capacitance matrix because the effect of the first equation of $(33)_1$ has been incorporated into the second equation of $(33)_2$ and the unknown potentials can be evaluated using the equation

$$[\boldsymbol{K}_{\text{eq}}]\{\boldsymbol{\phi}\} = \{0\}. \tag{34}$$

The unknown potentials in the piezolayers have been determined by taking the known potentials to the right-hand side and solving (34) , which is similar to the process of solving thermal problems where one knows temperatures on some nodes and the temperatures on the other nodes are evaluated. Once all the potentials are known, $(33)_1$ can be used to determine the displacements. The buckling eigenequation is (32).

## 3. Results and discussion

A finite element solver was written implementing the formulation above. In this section we discuss some validation tests and then new example calculations involving a system where neither plane stress nor plain strain conditions are assumed.

***Validation.*** The code was validated for electric buckling by comparison with the results in [Varelis and Saravanos 2004]. The same example was also subjected to a three-dimensional FE computation in ANSYS; due to the limitations of ANSYS, a thermal analog of the linear electrical buckling problem [Dong and Meng 2006] was solved as a proxy.

The example beam of Varelis and Saravanos is a three-layer [pzt/Al/pzt] composite with length 200 mm, width 20 mm, thickness of each piezo layer $t_p = 0.25$ mm, and aluminum layer thickness $t_a = 0.5$ mm. In the case $\alpha = 1$ (the beam is allowed to expand freely in the $y$ direction), we obtain these values for the critical electrical buckling voltage:

$$\begin{array}{rl} \text{present approach} & 189.6\,\text{V} \\ \text{ANSYS 3D model} & 188.8\,\text{V} \\ \text{[Varelis and Saravanos 2004]} & 188\quad\text{V} \end{array} \tag{35}$$

We observe good agreement between all three results.

For thermal buckling validation, we took an example beam from [Giannopoulos et al. 2007]: a three-layer [pzt/Al/pzt] composite with length 70 mm and width 5 mm. The thickness of each piezo layer is $t_p = 0.191$ mm and that of the aluminium layer is $t_a = 0.070$ mm. The beam is subjected to a uniform temperature rise above the ambient temperature, and again we take $\alpha = 1$. These are the values obtained for the critical thermal buckling temperature:

$$\begin{array}{rl} \text{present approach} & 29.7^\circ\text{C} \\ \text{ANSYS 3D model} & 28.3^\circ\text{C} \end{array} \tag{36}$$

No direct comparison is possible with the calculations in [Giannopoulos et al. 2007], since that reference only contains the thermal buckling analysis of plates. However, we performed a three-dimensional analysis in ANSYS for the same problem solved by these authors, and it was found that the ANSYS result and their result agree very well.

***Further examples.*** We next performed the thermal and electrical buckling analysis for an example structure taken from [Giannopoulos et al. 2007], using different assumptions for the parameter $\alpha$. In the particular cases of plane stress assumptions and plane strain assumptions, the results obtained are compared with those obtained with ANSYS; however, the more general case (neither plane stress nor plane strain) has also been studied.

The beam is a three layer [pzt/Al/pzt] composite with length 70 mm and width 5 mm. The thickness $t_p$ of each piezo layer is 0.191 mm and the aluminium layer thickness $t_a$ is 0.070 mm.

*Electrical buckling.* An equal voltage was applied to the piezolayers in the corresponding direction as shown in Figure 6, so that pure compression is developed in the structure due to the kinematic constraints imposed by the boundary conditions. The results obtained for the buckling voltage with our FE solver under assumptions of plane stress, plane strain, and free expansion ($\alpha = 1$) are shown here along with those obtained from an ANSYS solution of the thermal analog [Dong and Meng 2006] to our problem:

| | free expansion | plane stress | plane strain | |
|---|---|---|---|---|
| ANSYS (3D/2D/2D) | 98.3 V | 102.7 V | 78.4 V | (37) |
| present approach | 97.5 V | 102.3 V | 78.2 V | |

This shows good agreement between the ANSYS results and those from the present analysis; in particular, our critical buckling voltage calculated using $\alpha = 1$ (free expansion) matches closely the one obtained using a three-dimensional analysis in ANSYS.

It is also clear that the calculated critical buckling voltage varies greatly with the constraints assumed. This dependence was explored further by varying the value of $\alpha$ in the calculation using the present approach. For $\alpha = 1$ (free expansion), as we have seen, we obtained 97.5 V, then 91.8 V for $\alpha = 0.75$, and 86.7 V for $\alpha = 0.5$, 82.2 V for $\alpha = 0.25$, and finally 78.2 V, for $\alpha = 0$ (plane strain assumption). The decrease in the critical buckling voltage with $\alpha$ can be rationalized by observing that as $\alpha$ is reduced, compressive stress is increased in the $y$ direction (perpendicular to the plane of the FE model), which in turn increases the voltage produced in the piezo layer. The developed voltage is such that it causes the piezo layer to expand in the other two directions (in the plane of the FE model). This expansion causes additional compressive stress due to the imposed kinematic constrains on the boundary, which in turn makes the structure buckle at lower voltages.

We extended the computation to $\alpha < 0$, meaning that external strain is applied in compression (Figure 5, right), and to $\alpha > 1$, meaning that external strain is applied in tension (Figure 5, left). When $\alpha < 0$ the trend just discussed still holds true: the calculated critical buckling voltage decreases in tandem with $\alpha$. Thus for $\alpha < 0$ we have 74.6 V at $\alpha = -0.25$ and 71.3 V at $\alpha = -0.5$. When $\alpha > 1$ the critical buckling voltage increases (103.9 V at $\alpha = 1.25$ and 111.3 V at $\alpha = 1.5$); this is because the expansion in the $y$ direction produces voltage in such a way that the piezo layer contracts in the $xz$ plane. Due to the kinematic constraints imposed by the boundary condition, this produces tensile stress opposed to the compressive stress produced by electrical actuation, resulting in an increase in the buckling voltage.

*Thermal buckling.* The analysis carried out in the preceding paragraphs was repeated for thermal buckling. Here the setup as the same as in Figure 6, but there is no applied voltage. Instead, the beam is subjected to a uniform temperature rise above the ambient temperature. The buckling temperatures obtained in the calculations under various assumptions are as follows:

| | free expansion | plane stress | plane strain | |
|---|---|---|---|---|
| ANSYS (3D/2D/2D) | 28.30 °C | 29.62 °C | 22.56 °C | (38) |
| present approach | 29.66 °C | 29.66 °C | 22.44 °C | |

Again we see good agreement between the ANSYS calculations and those based on the present approach. Further, the calculations yield the same critical buckling temperature using the plane stress assumption or using $\alpha = 1$ (free expansion). This is because the thermal expansion mechanism is given by the initial strain vector $\{S_0\}$, which is not reduced under the plane stress assumption. More precisely, when the three-dimensional stress-strain relation (1) is reduced to a two-dimensional stress-strain relation based on the plane stress assumption ($T_2 = T_4 = T_6 = 0$, $D_2 = E_2 = 0$), the initial strain vector $\{S_0\}$ is unchanged.

Here are the results given by the present approach for various values of $\alpha$:

| | | | | | |
|---|---|---|---|---|---|
| $\alpha = -0.5$ | 19.9529°C | $\alpha = 0.25$ | 23.9296°C | $\alpha = 1$ | 29.6673°C |
| $\alpha = -0.25$ | 21.1288°C | $\alpha = 0.75$ | 27.4970°C | $\alpha = 1.5$ | 35.1063°C |
| $\alpha = 0$ | 22.4481°C | $\alpha = 0.5$ | 25.6004°C | $\alpha = 1.25$ | 32.1751°C |

We see that the critical buckling temperature increases with $\alpha$. This is because, as $\alpha$ decreases, the compressive stress in the direction perpendicular to the FE model increases, which makes the material expand in the other two directions due to the Poisson effect. This expansion causes additional compressive stress in the beam due to the kinematic constraints imposed by the boundary condition, reducing the critical buckling temperature. The influence of $\alpha$ on the critical buckling temperature is similar to that of the influence in critical buckling voltage as discussed earlier.

*Combined thermal and electrical buckling.* In the combined thermal and electrical buckling analysis, the critical electrical buckling voltage was predicted for different uniform temperature increases in the beam. All analyses carried out for electrical and thermal buckling were also repeated for combined thermal and electrical buckling. The results obtained under different assumptions are presented in Figure 7 (comparison with ANSYS calculation performed on the thermal analog [Dong and Meng 2006]) and in Figure 8 (dependence on $\alpha$). The results are similar to those just discussed.

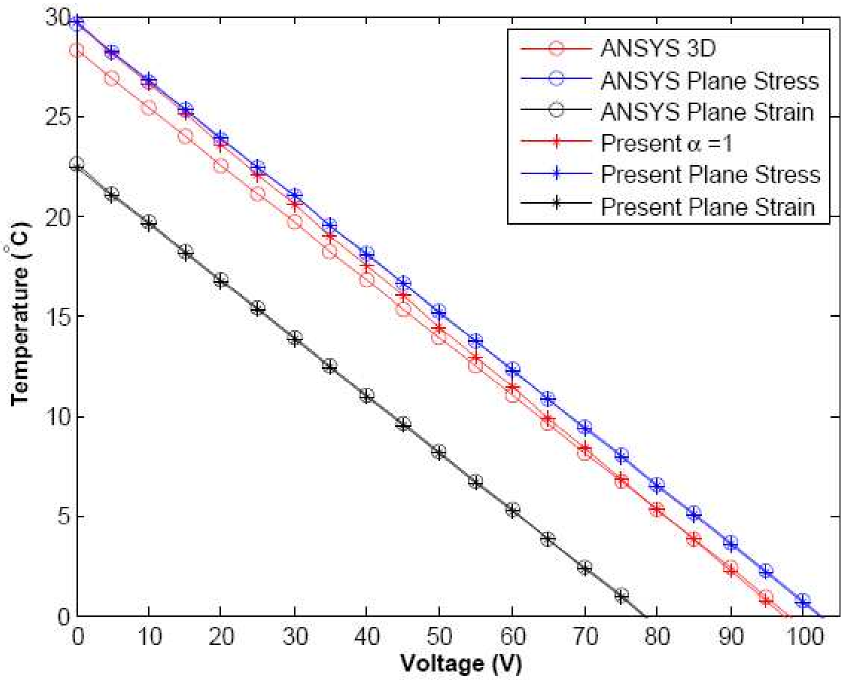


**Figure 7.** Values of critical buckling voltage obtained with the present approach and with ANSYS [Varelis and Saravanos 2004].

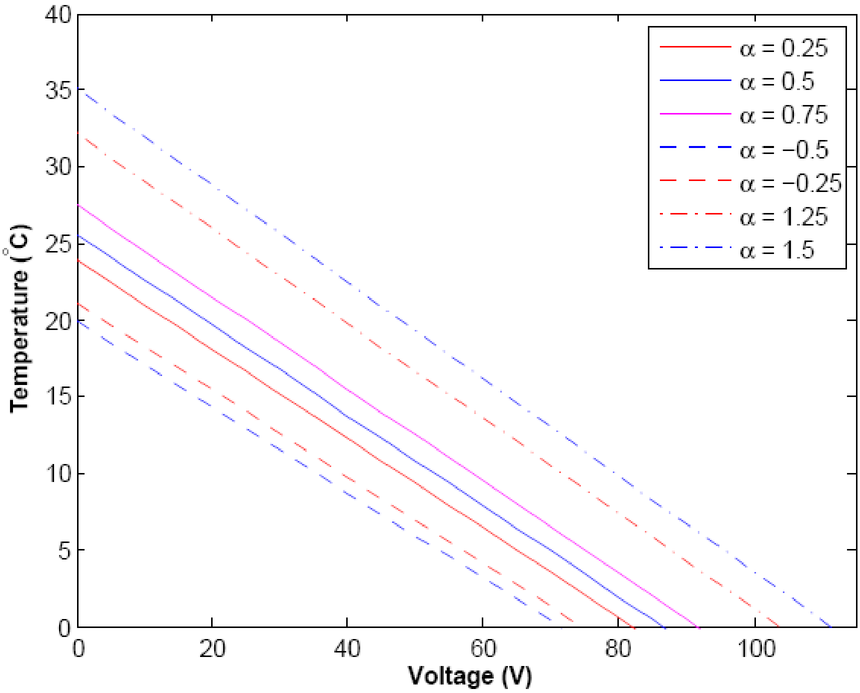


**Figure 8.** Influence of $\alpha$ on the combined thermal and electrical buckling analysis.

## 4. Conclusion

A generalized plane strain FE formulation was developed to predict the critical buckling voltage and critical buckling temperature of a piezo composite beam for cases other than those characterized by plane strain and plane stress assumptions. The two-dimensional FE formulation presented in this paper is capable of describing the strain $\varepsilon^0$ allowed/applied in the direction which is not included in the two-dimensional FE model, (here the $y$ direction) if the strain $\varepsilon^0$ is specified in terms of the free expansion strain $\varepsilon^0_{yy}$. An eight-node quadrilateral element was developed based on the new formulation, and the FE solver results were validated by comparison to the results in [Varelis and Saravanos 2004] and those obtained with ANSYS. These results are in good agreement with each other. The critical electrical and thermal buckling load for the cases other than those characterized by plane stress and plane strain, which can be handled by the present two-dimensional FE solver, was analyzed, and it was found that the influence of $\alpha$ on the critical buckling voltage as well as the critical buckling temperature is significant. Since the present formulation varies only in the constitutive equation matrix reduction, this formulation can be easily incorporated into the existing piezostructure coupled FE solvers.

## Acknowledgment

The authors acknowledge the painstaking efforts by the reviewers and the editor for improving the manuscript.

## References

[Allik and Hughes 1970] H. Allik and T. J. R. Hughes, "Finite element method for piezoelectric vibration", *Int. J. Numer. Methods Eng.* **2**:2 (1970), 151–157.

[Benjeddou 2000] A. Benjeddou, "Advances in piezoelectric finite element modeling of adaptive structural elements: a survey", *Comput. Struct.* **76**:1-3 (2000), 347–363.

[Cook et al. 2003] R. D. Cook, D. S. Malkus, M. E. Plesha, and R. J. Witt, *Concepts and applications of finite element analysis*, Wiley, New York, 2003.

[Dong and Meng 2006] X.-J. Dong and G. Meng, "Dynamic analysis of structures with piezoelectric actuators based on thermal analogy method", *Int. J. Adv. Manuf. Tech.* **27**:9-10 (2006), 841–844.

[Giannopoulos et al. 2007] G. Giannopoulos, F. Santafe, J. Monreal, and J. Vantomme, "Thermal, electrical, mechanical coupled mechanics for initial buckling analysis of smart plates and beams using discrete layer kinematics", *Int. J. Solids Struct.* **44**:14-15 (2007), 4707–4722.

[Hu and Pagano 1997] S. Hu and N. J. Pagano, "On the use of a plane-strain model to solve generalized plane-strain problems", *J. Appl. Mech.(ASME)* **64**:1 (1997), 236 – 238.

[Krueger et al. 2002] R. Krueger, I. L. Paris, T. K. O'Brien, and P. J. Minguet, "Comparison of 2D finite element modeling assumptions with results from 3D analysis for composite skin-stiffener debonding", *Compos. Struct.* **57**:1-4 (2002), 161–168.

[Lerch 1990] R. Lerch, "Simulation of piezoelectric devices by two- and three-dimensional finite elements", *IEEE Trans. Ultrason. Ferroelectr. Freq. Control* **37**:3 (1990), 233–247.

[Lin and Yi 1991] K. Y. Lin and S. Yi, "Analysis of interlaminar stresses in viscoelastic composites", *Int. J. Solids Struct.* **27**:7 (1991), 929–945.

[Tzou and Tseng 1990] H. S. Tzou and C. I. Tseng, "Distributed piezoelectric sensor/actuator design for dynamic measurement/control of distributed parameter systems: a piezoelectric finite element approach", *J. Sound Vib.* **138**:1 (1990), 17–34.

[Varelis and Saravanos 2002] D. Varelis and D. A. Saravanos, "Nonlinear coupled mechanics and initial buckling of composite plates with piezoelectric actuators and sensors", *Smart Mater. Struct.* **11**:3 (2002), 330–336.

[Varelis and Saravanos 2004] D. Varelis and D. A. Saravanos, "Coupled buckling and postbuckling analysis of active laminated piezoelectric composite plates", *Int. J. Solids Struct.* **41**:5-6 (2004), 1519–1538.

Received 23 Apr 2008. Revised 25 Sep 2008. Accepted 1 Oct 2008.

R. JEROME: jerrome_r@hotmail.com
*Department of Mechanical Engineering, Machine Design Section, Room No. 403, Indian Institute of Technology Madras, Chennai 600 036, India*

N. GANESAN: nganesan@iitm.ac.in
*Department of Mechanical Engineering, Machine Design Section, Room No. 405, Indian Institute of Technology Madras, Chennai 600 036, India*